NASA/TM—2012-217689

Advanced Materials and Component Development for Lithium-Ion Cells for NASA Missions

Concha M. Reid
Glenn Research Center, Cleveland, Ohio

September 2012

NASA STI Program . . . in Profile

Since its founding, NASA has been dedicated to the advancement of aeronautics and space science. The NASA Scientific and Technical Information (STI) program plays a key part in helping NASA maintain this important role.

The NASA STI Program operates under the auspices of the Agency Chief Information Officer. It collects, organizes, provides for archiving, and disseminates NASA's STI. The NASA STI program provides access to the NASA Aeronautics and Space Database and its public interface, the NASA Technical Reports Server, thus providing one of the largest collections of aeronautical and space science STI in the world. Results are published in both non-NASA channels and by NASA in the NASA STI Report Series, which includes the following report types:

- TECHNICAL PUBLICATION. Reports of completed research or a major significant phase of research that present the results of NASA programs and include extensive data or theoretical analysis. Includes compilations of significant scientific and technical data and information deemed to be of continuing reference value. NASA counterpart of peer-reviewed formal professional papers but has less stringent limitations on manuscript length and extent of graphic presentations.

- TECHNICAL MEMORANDUM. Scientific and technical findings that are preliminary or of specialized interest, e.g., quick release reports, working papers, and bibliographies that contain minimal annotation. Does not contain extensive analysis.

- CONTRACTOR REPORT. Scientific and technical findings by NASA-sponsored contractors and grantees.

- CONFERENCE PUBLICATION. Collected papers from scientific and technical conferences, symposia, seminars, or other meetings sponsored or cosponsored by NASA.

- SPECIAL PUBLICATION. Scientific, technical, or historical information from NASA programs, projects, and missions, often concerned with subjects having substantial public interest.

- TECHNICAL TRANSLATION. English-language translations of foreign scientific and technical material pertinent to NASA's mission.

Specialized services also include creating custom thesauri, building customized databases, organizing and publishing research results.

For more information about the NASA STI program, see the following:

- Access the NASA STI program home page at *http://www.sti.nasa.gov*

- E-mail your question to *help@sti.nasa.gov*

- Fax your question to the NASA STI Information Desk at 443–757–5803

- Phone the NASA STI Information Desk at 443–757–5802

- Write to:
  STI Information Desk
  NASA Center for AeroSpace Information
  7115 Standard Drive
  Hanover, MD 21076–1320

NASA/TM—2012-217689

Advanced Materials and Component Development for Lithium-Ion Cells for NASA Missions

Concha M. Reid
Glenn Research Center, Cleveland, Ohio

Prepared for the
Energy Tech 2012
sponsored by the Institute of Electrical and Electronics Engineers
Cleveland, Ohio, May 29–31, 2012

National Aeronautics and
Space Administration

Glenn Research Center
Cleveland, Ohio 44135

September 2012

Acknowledgments

All of the work presented in this paper was funded by the National Aeronautics and Space Administration, Enabling Technology Development and Demonstration Program High Efficiency Space Power Systems Project (formerly the Exploration Technology Development Program, Energy Storage Project). Numerous people participated in the synthesis of materials, generation of data, and interpretation of results. Contributions from Richard Baldwin, William Bennett and Brianne Scheidegger, NASA Glenn Research Center; Judith Jeevarajan, NASA Johnson Space Center; and William West, Marshall Smart, Kumar Bugga, and Jessica Soler, NASA Jet Propulsion Lab are gratefully acknowledged. Contributors via efforts funded through NASA Research Announcement NNC08ZP022N include the following: Nader Hagh and Ganesh Skandan; NEI Corporation; Arumugam Manthiram, University of Texas at Austin; Christopher Lang, Physical Sciences, Inc.; Justin Golightly, Lockheed Martin Space Systems Company; Gleb Yushin, Georgia Institute of Technology; Igor Luzinov, Clemson University; Boris Ravdel, Yardney Technical Products; Brett Lucht, University of Rhode Island, and support staff at these companies and universities.

Level of Review: This material has been technically reviewed by technical management.

Available from

NASA Center for Aerospace Information
7115 Standard Drive
Hanover, MD 21076–1320

National Technical Information Service
5301 Shawnee Road
Alexandria, VA 22312

Available electronically at http://www.sti.nasa.gov

Advanced Materials and Component Development for Lithium-Ion Cells for NASA Missions

Concha M. Reid
National Aeronautics and Space Administration
Glenn Research Center
Cleveland, Ohio 44135

Abstract

Human missions to Near Earth Objects, such as asteroids, planets, moons, liberation points, and orbiting structures, will require safe, high specific energy, high energy density batteries to provide new or extended capabilities than are possible with today's state-of-the-art aerospace batteries. The Enabling Technology Development and Demonstration Program, High Efficiency Space Power Systems Project battery development effort at the National Aeronautics and Space Administration (NASA) is continuing advanced lithium-ion cell development efforts begun under the Exploration Technology Development Program Energy Storage Project. Advanced, high-performing materials are required to provide improved performance at the component-level that contributes to performance at the integrated cell level in order to meet the performance goals for NASA's High Energy and Ultra High Energy cells. NASA's overall approach to advanced cell development and interim progress on materials performance for the High Energy and Ultra High Energy cells after approximately 1 year of development has been summarized in a previous paper. This paper will provide an update on these materials through the completion of 2 years of development. The progress of materials development, remaining challenges, and an outlook for the future of these materials in near term cell products will be discussed.

1.0 Introduction

NASA is developing High Energy (HE) and Ultra High Energy (UHE) advanced lithium-ion (Li-ion) cells with the goals of attaining specific energies of 180 watt-hours per kilogram (Wh/kg) and 260 Wh/kg, respectively, when measured at C/10 and 0 °C, in cells that are inherently safe. The HE cell goals are being addressed through the development of advanced cathode components, flame retardant electrolytes, safety devices, and optimized cell designs. The newly developed components will be combined with a commercial graphite anode from Mitsubishi Chemical Corporation (MPG-111) that can achieve a specific capacity of 330 milliampere-hours per gram (mAh/g) at C/10 and 0 °C and a commercial battery-grade separator to comprise an HE cell design. The UHE cell goals will be achieved through the development of advanced anodes and combining them with the cathode, safety device, and separator utilized in the HE cell. A flame retardant electrolyte specially formulated to be compatible with the advanced anode will be used in the UHE cell design. Background information on the cell chemistries, their components, and cell designs are documented in prior papers by Reid and Bennett and by Reid (Refs. 1 and 2).

A table of Key Performance Parameters (KPPs) is shown in Table 1. These KPPs establish target criteria for the performance of cell components and Li-ion cells, and project the expected performance of a battery-level system comprised of the cells under development. State-of-the art (SOA) is based on aerospace design Li-ion cells and batteries developed by Yardney Technical Products for operation on the Mars Exploration Rovers (MER).

TABLE 1.—KEY PERFORMANCE PARAMETERS

Performance parameter	State of the Art	Current value	Threshold value[a]	Goal[a]
No fire or flame	Instrumentation/controllers used to prevent unsafe conditions. There is no non-flammable electrolyte in SOA	Preliminary results indicate a small reduction in performance using safer electrolytes and cathode coatings	Tolerant to electrical and thermal abuse such as over-temperature, over-charge, reversal, and short circuits with no fire or thermal runaway[c]	Tolerant to electrical and thermal abuse such as over-temperature, over-charge, reversal, and short circuits with no fire or thermal runaway[c]
Battery-level specific energy,[b] (Wh/kg)	90 Wh/kg at C/10 and 30 °C 83 Wh/kg at C/10 and 0 °C (MER rovers)	160 at C/10 and 30 °C (HE) 170 at C/10 and 30 °C (UHE) 80 Wh/kg at C/10 and 0 °C (predicted)	135 Wh/kg at C/10 and 0 °C "High-Energy" 150 Wh/kg at C/10 and 0 °C "Ultra-High Energy"	150 Wh/kg at C/10 and 0 °C "High-Energy" 220 Wh/kg at C/10 and 0 °C "Ultra-High Energy"
Cell-level specific energy, (Wh/kg)	130 Wh/kg at C/10 and 30 °C 118 Wh/kg at C/10 and 0 °C	199 at C/10 and 23 °C (HE) 213 at C/10 and 23 °C (UHE) 100 Wh/kg at C/10 and 0 °C (predicted)	165 Wh/kg at C/10 and 0 °C "High-Energy" 180 Wh/kg at C/10 and 0 °C "Ultra-High Energy"	180 Wh/kg at C/10 and 0 °C "High-Energy" 260 Wh/kg at C/10 and 0 °C "Ultra-High Energy"
Cathode-level specific capacity, (mAh/g)	180 mAh/g	252 mAh/g at C/10 and 25 °C 190 mAh/g at C/10 and 0 °C	260 mAh/g at C/10 and 0 °C	280 mAh/g at C/10 and 0 °C
Anode-level specific capacity, (mAh/g)	280 mAh/g (MCMB)	330 at C/10 and 0 °C (HE) 1200 mAh/g at C/10 and 0 °C for 10 cycles (UHE)	600 mAh/g at C/10 and 0 °C "Ultra-High Energy"	1000 mAh/g at C/10 0 °C "Ultra-High Energy"
Battery-level energy density	250 Wh/l	n/a	270 Wh/l "High-Energy" 360 Wh/l "Ultra-High"	320 Wh/l "High-Energy" 420 Wh/l "Ultra-High"
Cell-level energy density	320 Wh/l	n/a	385 Wh/l "High-Energy" 460 Wh/l "Ultra-High"	390 Wh/l "High-Energy" 530 Wh/l "Ultra-High"
Operating temperature	–20 to +40 °C	0 to +30 °C	0 to 30 °C	0 to 30 °C

[a]Assumes prismatic cell packaging for threshold values. Goal values include lightweight battery packaging.
[b]Battery values are assumed at 100% depth-of-discharge (DoD), discharged at C/10 to 3.0 volts/cell, and at 0 °C operating conditions.
[c]Over-temperature up to 110 °C; reversal 150% excess discharge at 1C; pass external and simulated internal short tests; overcharge 100% at 1C for Goal and 80% at C/5 for Threshold Value.

NASA Research Announcement (NRA) contracts that were initiated specifically to develop components targeted for the HE and UHE cells have concluded after a two-year period of effort. Electroactive materials, electrodes, sample coupons, and electrolytes were delivered to NASA at intervals of 6, 11, 18, and 23 months (mo.) into their development and were independently assessed by NASA Glenn Research Center (GRC), Johnson Space Center (JSC), and/or Jet Propulsion Laboratory (JPL) according to standard procedures established for this development project. These materials will be referred to as 6, 11, 18, and 23 mo. deliverables/materials. The progression of the performance of the materials over the development timeframe will be discussed in this paper. Comparisons of the materials' performance relative to the goal values will be discussed, parameters that are on target with the goal criteria will be highlighted, and areas where technical advancement is still required will be identified. Additionally, projected characteristics of cells incorporating these materials will be presented.

2.0 High Energy Cell

2.1 Cathodes

Advanced cathodes are critical to the development of high specific energy HE and UHE cells. Layered transition metal oxide materials containing lithium, nickel, manganese, and cobalt ($Li[LiNMC]O_2$) are being developed with the goal to attain 280 mAh/g when discharged at C/10 and 0 °C to 3.0 volts (V). The cathode materials discussed in this paper were developed at the University of Texas at Austin (UTA) and at NEI Corporation (NEI).

UTA's focus has been to systematically investigate solid solutions of $(1\text{-}z)[Li_{1/3}Mn_{2/3}]O_2\text{-}zLi[Ni_{1\text{-}x\text{-}y}Mn_xCo_y]O_2$ to identify and optimize lithium-rich, layered compositions that can meet the goals stated above. The composition $Li[Li_{0.2}Mn_{0.54}Ni_{0.13}Co_{0.13}]O_2$ was targeted as the stoichiometry that could potentially offer the desired specific capacity. Improvement in irreversible capacity loss (ICL) (reduction of), discharge capacity, and rate capability were achieved through surface modifications (e.g., application of coatings) using solution-based processes and blending the base material with lithium-free insertion hosts (Ref. 3). NEI's approach to cathode development has been the design and synthesis of two-dimensional layered electrodes based on a composite of $Li[Li_{1/3}Mn_{2/3}]O_2$ and $Li[Mn_{1/3}Ni_{1/3}Co_{1/3}]O_2$ (Ref. 4).

UTA and NEI materials were independently assessed at NASA JPL using a standard set of test conditions in 2032-type coin cell half cells with a Li metal electrode, 1.0 molar (M) lithium hexafluorophoshate ($LiPF_6$) in ethylene carbonate:diethyl carbonate:dimethyl carbonate (EC:DEC:DMC) electrolyte in a 1:1:1 ratio by volume (baseline electrolyte), and a 20 micron (μm) thick Tonen Setela (Toray Tonen) separator, unless otherwise noted. Cathode test procedures are given in Table 2.

The performance against key metrics that are fundamental to the overall characterization of the cathodes has been exhibiting gradual improvement over the course of 2 years. The "best" values demonstrated for these parameters are compared to the goal values on the "spider plot" shown in Figure 1. Best values are defined as the highest value of the particular parameter achieved over the two-year development period. Hence, values are not necessarily for the same material. Table 3 quantitatively lists the best and goal values and the materials from which the best values were measured. In addition, it lists the values of all the parameters for the most recent deliverables from each developer. Values reported are for the average of four cells, with the exception of the UTA 11 mo. material, whose value is the average of two cells. The parameters shown include first cycle reversible capacity, specific capacity, temperature performance, tap density, rate capability, and cycle life. The following paragraphs describe the data for these parameters in more detail.

TABLE 2.—CATHODE TEST PROCEDURES

Test stage	Test conditions
Formation	At 23 °C, charge at C/20 to 4.8 V, hold voltage, and allow current to taper to C/50. Rest for 15 min. Discharge at C/20 to 2V. Perform for 5 cycles.
20 °C Characterization	At 20 °C, charge at C/10 to 4.8 V, hold voltage, and allow current to taper to C/50. Rest for 15 min. Discharge at C/10 to 2V. Perform for 10 cycles.
0 °C Characterization	First charge is performed at 20 °C. All other charges are performed at 0 °C. Charge at C/10 to 4.8 V, hold voltage, and allow current to taper to C/50. Rest for 15 min. Soak for a minimum of 2 hours after a temperature change. At 0 °C, discharge at C/10 to 2V. Perform for 10 cycles.
30 °C Characterization	Soak at 30 °C for a minimum of 2 hours after a temperature change. Charge at C/10 to 4.8 V, hold voltage, and allow current to taper to C/50. Rest for 15 min. Discharge at C/10 to 2V. Perform for 10 cycles.

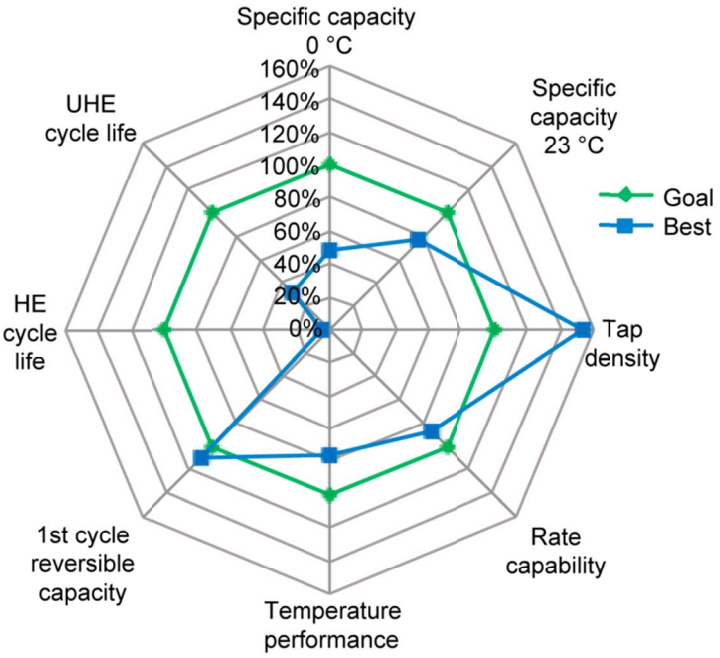

Figure 1.—Cathode best values as compared to goal values.

TABLE 3.—SUMMARY OF CATHODE BEST VALUES AND LATEST VALUES

Metric	Goal	Best values		Values for latest materials	
		Value	Material	UTA 23 mo. coated	NEI 23 mo. uncoated
First cycle reversible capacity (%)	81	87	UTA 18 and 23 mo. coated	87	65
Specific capacity, RT, C/10 to 3V (mAh/g)	311	238	UTA 11 mo. uncoated	164	191
Specific capacity, 0 °C, C/10 to 3V (mAh/g)	280	135	UTA 11 mo. coated	126	130
RT capacity retention at 0 °C (%)	90	72	UTA 23 mo. coated	85	72
Tap density (g/cc)	≥1.5	>2.3	NEI and UTA, both 18 mo. uncoated	2.02	1.34
Rate capability at C/5 as compared to C/10 (%)	95	83	NEI 6 mo. uncoated	Not measured	Not measured
Projected cycle life for HE (cycles to 80% of initial capacity)	2000	81	UTA	Not measured	Not measured
Projected cycle life for UHE (cycles to 80% of initial capacity)	250	81	UTA	Not measured	Not measured

2.1.1 Reversible Capacity

First-cycle reversible capacity is measured on the initial formation cycle. The percentage of first cycle reversible capacity is equivalent to (100 percent minus the percentage of first-cycle ICL) as the cell is cycled between 2.0 V and 4.8 V, where percent ICL is given by the following equation:

$$\%\, ICL = \frac{charge - discharge}{discharge} \times 100,$$ where *charge* = charge capacity, and *discharge* = discharge capacity

The goal for first cycle reversible capacity is 81 percent, or inversely, the first cycle ICL should ideally be no greater than 19 percent. This value is based on typical results for the first cycle reversibility of lithium nickel cobalt aluminum oxide, a standard lithium-ion cathode material, and was verified by internal NASA measurements. The UTA Li[LiNMC]O_2 materials have exhibited a first cycle reversible capacity of 87 percent. Changes to synthesis techniques and coating chemistry were instrumental in

improving the reversible capacity from the 50 to 75 percent values exhibited in early deliverables to NASA.

2.1.2 Specific Capacity

Specific capacity at 20 and 0 °C are plotted as a percentage of the specific capacity goals at C/10 and 3.0 V and the respective temperature. Specific capacity at 20 °C is reported for the first cycle following formation. Discharge was continued to 2.0 V and values were measured and reported at 3.0 V. Studies performed internally at NASA JPL have shown that there is a slightly higher rate of capacity fade with certain $Li[LiNMC]O_2$ materials when they are cycled between 4.7 and 2.0 V as opposed to between 4.7 and 3.0 V. However, cycling to 2.0 V provides valuable information on the residual capacity remaining between 3.0 and 2.0 V.

The best specific capacity measured at 20 °C and C/10 from 4.7 to 3.0 V is 238 mAh/g, which is 77 percent of the goal value of 311 mAh/g. Since project goals were established for 0 °C operation, the room temperature (RT) goal was derived from the 0 °C specific capacity goal, based on the desire to retain at least 90 percent of RT capacity when operating at 0 °C. In this paper, temperatures between 20 and 23 °C are considered RT.

Testing at 0 °C is performed after cycling ten times at 20 °C. Specific capacity at 0 °C is reported for the first discharge at 0 °C, after a charge at 20 °C. As with the 20 °C cycling, discharge was continued to 2.0 V and values were measured and reported at 3.0 V. At 0 °C and C/10 from 4.7 to 3.0 V, 135 mAh/g was obtained, only 48 of the goal value of 280 mAh/g. Since capacity at 0 °C is measured on the 11th operational cycle (after 20 °C cycling), some capacity fade occurred prior to obtaining the measurement at 0 °C. Experimentally, an 18-24 mAh/g decrease was typically observed from the first 20 °C discharge to the tenth 20 °C discharge. If the specific capacity delivered at 0 °C is adjusted for the capacity loss due to earlier cycling, the value approaches 57 percent of the goal.

2.1.3 Temperature Performance

Temperature performance is measured as the percentage of RT capacity retained at 0 °C. Excessive capacity loss at lower temperatures can limit the practical design of a battery that must operate at those temperatures. In such a case, in order to supply enough operational capacity, a battery may need to be oversized to compensate for the decrease in delivered capacity at low temperatures. Alternately, thermal management must be designed in as part of the battery system to maintain the operating point at a warmer temperature. Either of these options may increase the mass of the battery system unless the battery load can be handled as part of a larger, integrated thermal management system, for example, as part of a vehicle's thermal management system.

Nonetheless, it is desirable to retain as much of the RT capacity when operating at 0 °C as possible. A goal of 90 percent was established for temperature performance based on what is reasonably practical given current SOA Li-ion cell performance. The specific capacity goals discussed in the previous section already take into account a 10 percent difference in temperature performance from 20 to 0 °C. Therefore, if 0 °C goals are met yet temperature performance is <90 percent, it is acceptable since in such a case the 20 °C performance would exceed its goal.

2.1.4 Tap Density

Tap density (TD), a measure of how well powders are able to be packed closely together, is a key attribute to measure in the determination of a material's suitability for the fabrication of cathodes from raw powders. To determine tap density, powders are placed in a graduated cylinder and taps are applied by automated equipment to compress the powder. The mass per unit volume is then measured on the compressed sample. The TD of the powders should ideally be $\geq$ 1.5-1.6 grams per cubic centimeter (g/cc) for manufacturability of cathodes of practical thickness on production equipment at Saft America, NASA's industrial partner for building HE and UHE cells.

Low tap density also impedes a material's ability to achieve high energy density, independently of production processes (Ref. 13). Materials that do not compress well contain more air between their particles, so they have high porosity when packed. These materials are unable to highly loaded (loading = capacity per unit area), since not enough material can occupy a unit area, resulting in low energy density.

2.1.5 Rate Capability

Rate capability is a measure of a material's ability to charge and/or discharge at specified currents. Rate capability was not routinely measured on cathodes. Studies were performed on early materials (NEI 6 mo.) to baseline the rate performance of this class of layered $Li[LiNMC]O_2$ materials. There is no specific requirement for rate capability at C/5 as compared to C/10 for the HE and UHE cells. However, for practical operation in a cell, the cathode should retain a significant portion of the C/10 capacity when operating at C/5. A target of 95 percent of the C/10 performance was set for the C/5 performance.

2.1.6 Cycle Life

Cycle life is the amount of cycles a cell delivers under specified conditions. Cycle life can vary depending upon how an electrode/cell is utilized. For these materials, the cycle life goals specify that the cathode should deliver at least 250 cycles until the point that 80 percent of its initial capacity is reached. Cycle life assessments are only performed on materials that demonstrate acceptable characteristics in other areas, however, NASA has collected limited data on selected deliverables to baseline this performance. Eighty-one cycles to 80 percent of initial capacity were projected from 60 cycles of data collected on experimental coated materials tested in coin cell half cells at UTA. A constant per cycle decrease in ampere-hour capacity was used for this projection.

Literature reports similar trends in capacity fade for this class of materials. Li et al. report 80 cycles to 80 percent of first cycle capacity when cycling at C/5 at 20 °C between 4.8 and 2.5 V (Ref. 5). They show that a rapid decrease in capacity occurs within the first 30 cycles, then the rate of fade decreases substantially for 70 more cycles. This is similar to the effect seen in some UTA coated materials. Li et al. also observed that this rapid decrease in capacity during early cycling occurred independently of discharge rate.

NEI also reports rapid fade in their "V2" materials (11 and 18 mo. deliverables) during early cycling before cycling stabilizes (Ref. 6). Hagh et al., attribute this phenomenon to an impedance rise rather than to intrinsic capacity loss. This suggests that if the impedance rise mechanism that occurs in early cycling can be overcome, less fade and better cycling stability can be obtained, which will extend cycle life.

2.1.7 Discussion

While NMC materials have potential to offer much higher specific capacity than traditional Li-ion cathodes such as lithium cobalt oxide ($LiCoO_2$), the $Li[Li_{1/3}Mn_{2/3}]O_2$ component of the NMC material has insulating properties that impacts its electronic conductivity. Additionally, a thick SEI layer is formed at the higher operating voltages, leading to slow kinetics and impacting the rate of lithium ion diffusion and charge transfer. These factors all lead to lower rate capability in the NMC cathode than is typically seen with other Li-ion chemistries (Ref. 14). Temperature performance is also much worse with NMC materials than with other lithium-ion chemistries, attributable to slow kinetics at low temperatures.

Figure 2 and Figure 3 contain spider plots that show the progression of the material properties as measured by the parameters discussed above for 6, 11, 18, and 23 mo. materials from UTA and NEI. Values plotted in each graph pertain to a single material. Although clear progress in materials development has been demonstrated over the past 2 years, component performance has still not achieved the goals necessary to enable the performance targets for the HE and UHE cells. For cathodes, most notably, specific capacity and cycle life are well below necessary targets. Results for specific capacity versus cycle number for representative materials delivered from each company are shown in Figure 4.

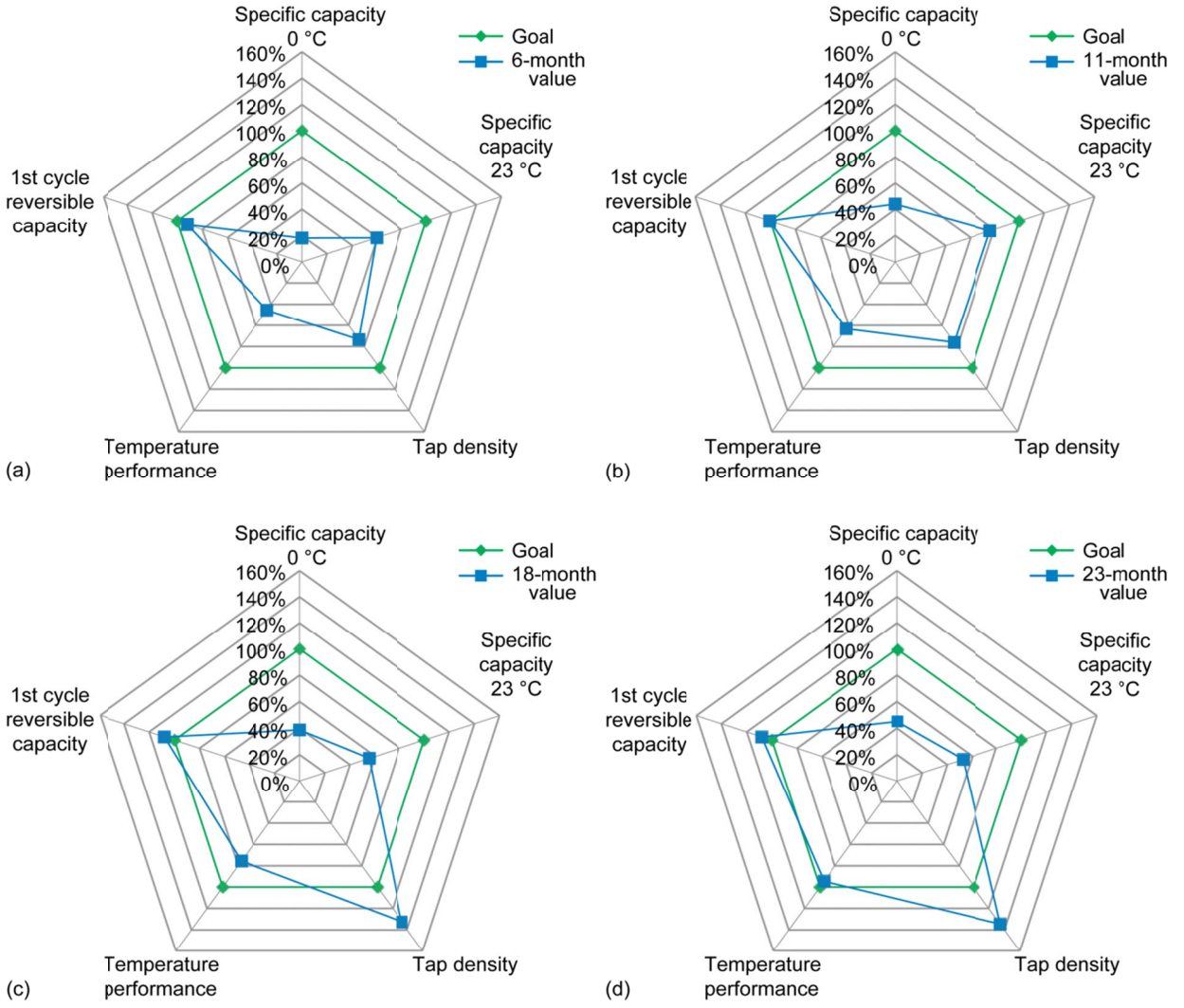

Figure 2.—Values of UTA key cathode parameters as a function of elapsed time into development. (a) Results after 6 months of development. (b) Results after 11 months of development. (c) Results after 18 months of development. (d) Results after 23 months of development.

Throughout the development of NMC cathode materials, performance of some parameters suffered from one delivery period to the next while the developer focused upon improvement in other parameters. This is most evident in the 18 mo. materials. During analysis of early materials, manufacturability studies revealed that TD was too low to allow for the production of viable cathodes. Hence, at UTA, efforts were refocused to utilize cathode material synthesis methods that would yield materials with higher TD. The first of these deliverables was received at 18 mo. Hydroxide precipitation synthesis procedures combined with non-destructive blending of precipitated precursors were used to formulate materials with TD ranging from 1.8 to 2.3 g/cc (Ref. 3).

NEI improved the TD of their 18 and 23 mo. materials via micro-structural modifications. They altered the particle morphology from irregular particles to uniform spherical particles that provided higher packing density (Ref. 4). Experimentation with different annealing atmospheres (other than an air environment) also resulted in TD improvements.

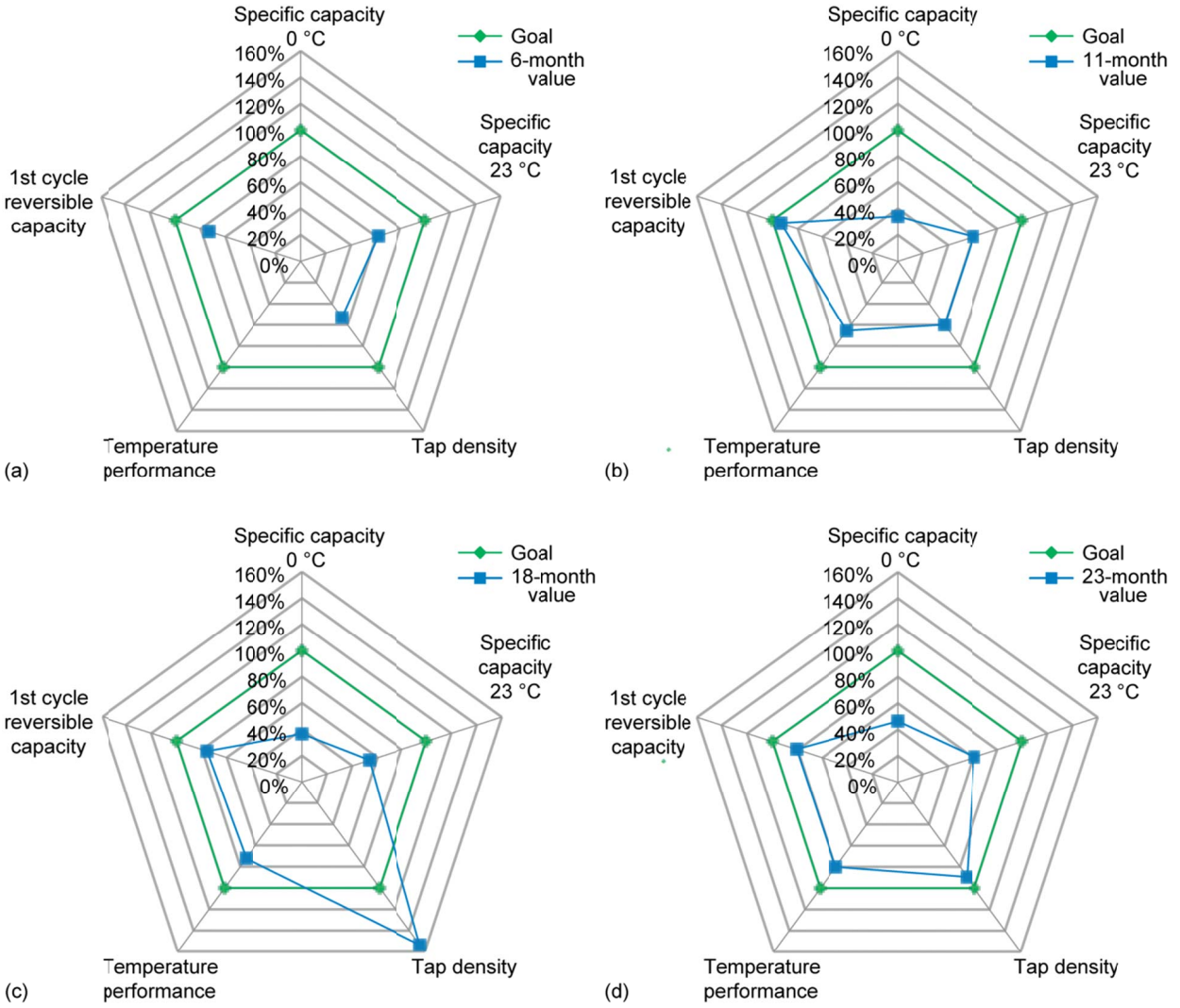

Figure 3.—Values of NEI key cathode parameters as a function of elapsed time into development. (a) Results after 6 months of development. (b) Results after 11 months of development. (c) Results after 18 months of development. (d) Results after 23 months of development.

Although experimentation with alternative synthesis techniques, particle morphology, and annealing atmospheres resulted in materials with higher TD, these materials exhibited lower specific capacity than had previously been demonstrated. Measurements performed at NEI on the higher TD materials revealed that they suffered from noticeably lower surface area than their lower TD counterparts. High surface area is favorable to electrochemical performance in that it provides a larger electrode-electrolyte interface and facilitates the charge transfer process of lithium ions (Refs. 7 and 8). The low surface area observed in the higher TD materials negatively impacted the electrochemical performance of the materials, resulting in lower specific capacity.

Optimizations were subsequently performed at UTA and NEI to maximize specific capacity while maintaining tap density at or above the minimum required for manufacturability. The achievement of the combination of the attributes discussed above in one material is critical for the success of the HE and UHE cell chemistries.

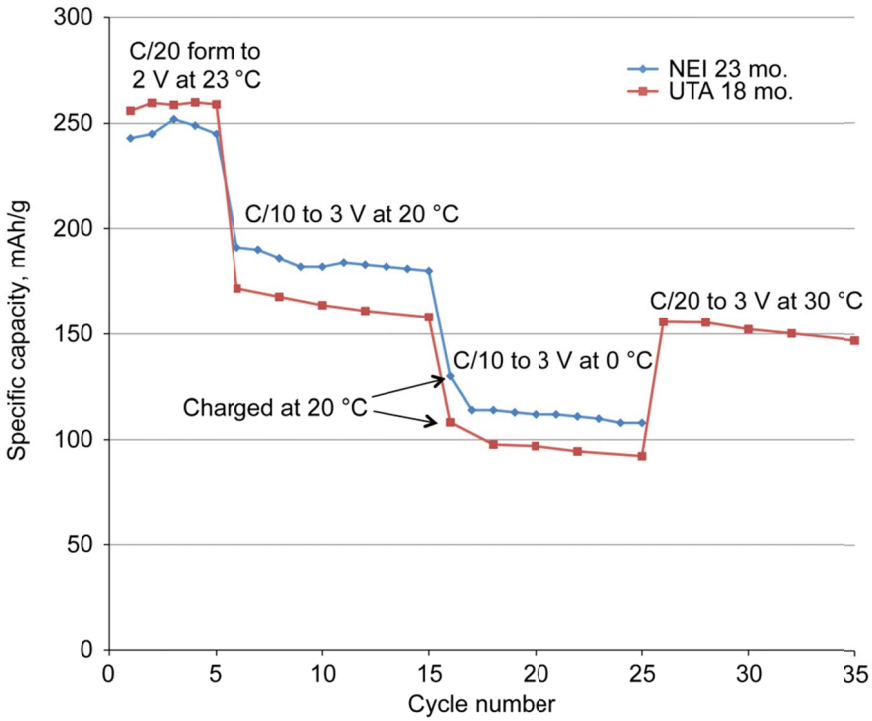

Figure 4.—Specific capacity versus cycle number for NEI and UTA Li[LiNMC]O_2 cathodes. Data was collected at NASA JPL.

2.2 Electrolytes

The HE and UHE cells require a safe electrolyte that is compatible with the electrode couples for these specific cell designs. In addition to its safety characteristics, the electrolyte must offer excellent ionic conductivity between 0 and 30 °C, provide electrochemical performance that enables project performance goals such as capacity and cycling stability, must be stable at voltages up to 5.0 V, and must facilitate the formation of stable solid electrolyte interphase (SEI) layers on the electrode surfaces.

In a previous paper, the flame-retardant and self-extinguishing properties of several experimental electrolyte formulations was presented (Ref. 2). Electrolytes containing triphenyl phosphate (TPP) concentrations between 5 and 15 percent and dimethyl methyl phosphonate (DMMP) concentration of 15 and 20 percent were demonstrated to self-extinguish faster than carbonate-based electrolytes in flame tests. In this paper, the electrochemical performance of candidate electrolytes with flame-retardant additives and their compatibility with the HE and UHE chemistries are discussed.

This section reports on the electrolyte development efforts at NASA JPL and at Yardney Technical Products/University of Rhode Island (YTP/URI) under their contract with NASA. It summarizes the extensive findings of the FY10 Final Report on electrolyte development issued to NASA GRC, authored by Smart et al. at NASA JPL (Ref. 9). Experimental electrolytes were tested in three-electrode, O-ring sealed, glass cells containing spiral rolls of MCMB-carbon anodes, $LiNiCoO_2$ cathodes, and lithium reference electrodes separated by two layers of Tonen Setela porous polypropylene separator, unless otherwise noted.

In a previous paper (Ref. 2), it was reported that YTP/URI electrolytes containing 15 and 20 percent DMMP [1.0M (95% $LiPF_6$ + 5% lithium bis(oxalato) borate (LiBOB)) in ethylene carbonate:ethyl methyl carbonate:dimethyl methyl phosphonate (EC:EMC:DMMP) in a 30:55:15 ratio and 1.0M (95% $LiPF_6$ + 5% LiBOB) in EC:EMC:DMMP in a 30:50:20 ratio] were demonstrated to have the lowest self-extinguishing times (SETs) of the electrolyte formulations tested, which included carbonate-based and TPP-containing carbonate blends. The DMMP-containing blends exhibited SETs of 1.8 and 0.4 sec, respectively, as compared to an SET of 33.4 sec for the all-carbonate electrolyte.

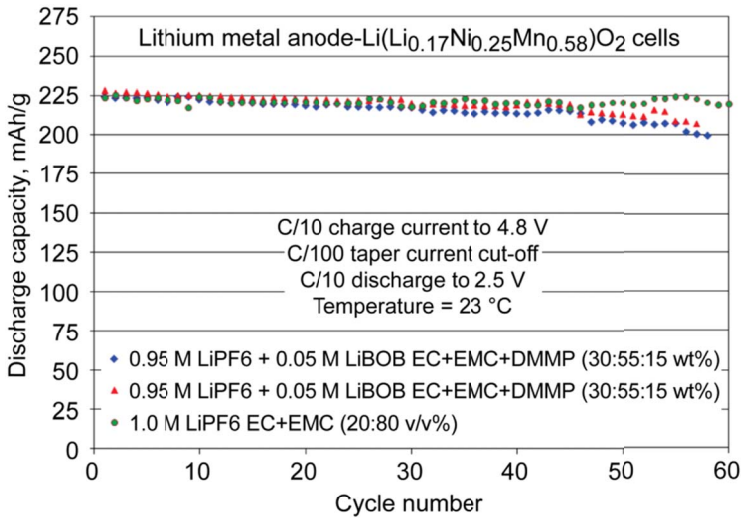

Figure 5.—Cycling performance of Li/Li^+-$Li(Li_{0.17}Ni_{0.25}Mn_{0.58})O_2$ cells with YTP/URI DMMP-containing electrolytes as compared to an all carbonate-based formulation. Data was collected at NASA JPL.

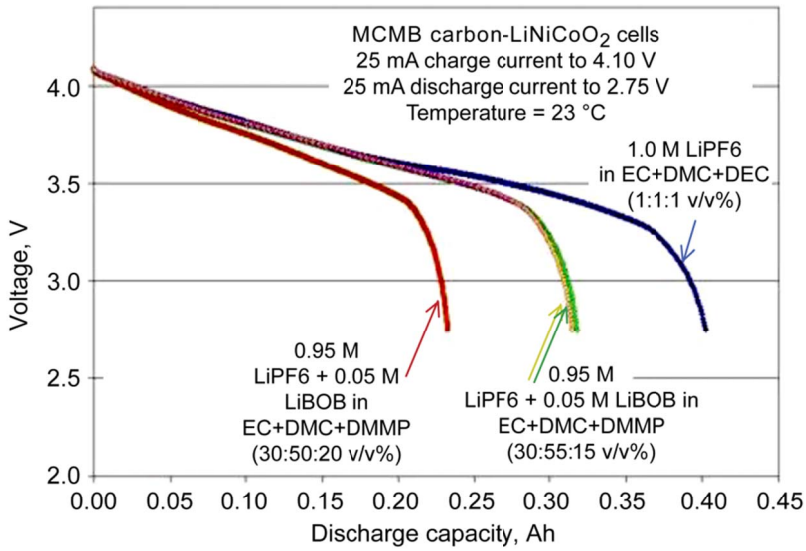

Figure 6.—Discharge capacity of MCMB-$LiNiCoO_2$ cells with YTP/URI DMMP-containing electrolytes as compared to an all carbonate-based formulation. Data was collected at NASA JPL.

In addition to their superior flame retardant properties, the YTP/URI electrolytes displayed good rate capability over a wide temperature range due to favorable cathode kinetics. Good low-temperature and cycle life performance were also observed. Additionally, in half-cells containing a high voltage cathode versus Li/Li+, these electrolytes were observed to offer excellent performance, comparable to the performance observed from the all-carbonate electrolyte control (Fig. 5). This exceptional performance at high voltages is attributed to the addition of LiBOB (Ref. 2).

Despite the promising performance discussed above, the performance of the electrolytes that contain DMMP was quite poor when cycled in cells containing carbon-based anodes such as mesocarbon micro-beads (MCMB) and MPG-111. Low capacity, poor efficiency, and high ICL were observed when the YTP/URI electrolytes were cycled in cells with MCMB and $LiNiCoO_2$, as seen in Figure 6. The data

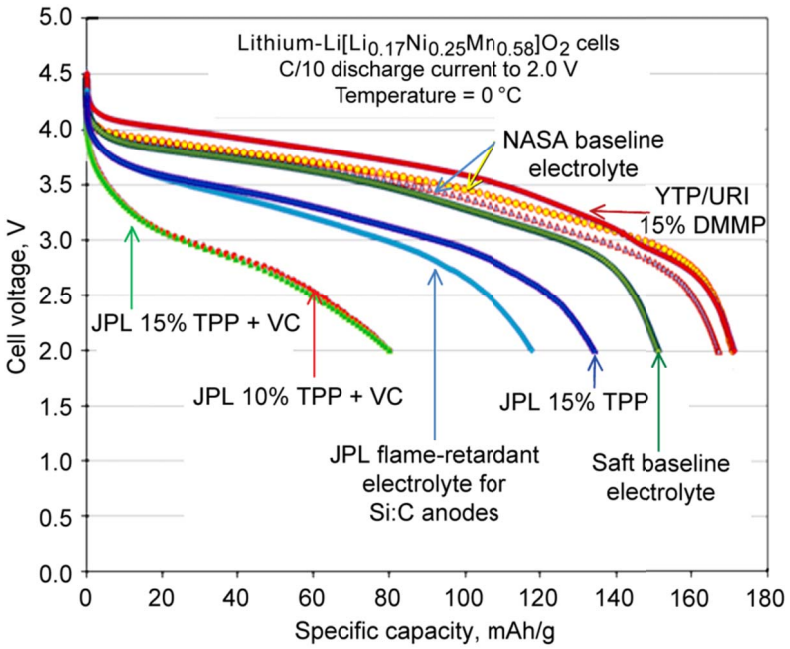

Figure 7.—Discharge performance of different electrolyte formulations. Data was collected at NASA JPL.

shown represents the 5th formation cycle, using a C/16 rate. Cells with electrolytes containing 15 percent DMMP on average yielded 78 percent of the capacity of the cells containing the baseline electrolyte, while cells with electrolyte containing 20 percent DMMP delivered only slightly more than half the capacity of the cells containing the baseline electrolyte. The addition of DMMP is thought to have caused excessive reactivity at the anode, which led to non-ideal SEI layer formation. This incompatibility of DMMP-containing electrolytes with carbon-based anodes precludes their use in the HE cell.

In alternative electrolyte formulations developed at NASA JPL, vinylene carbonate (VC), an SEI-promoting additive, was included in order to inhibit excessive reactivity and enhance SEI formation. Although VC was observed to benefit cathode kinetics in lower voltage systems, its incorporation into the selected electrolytes appeared to have a detrimental effect in high voltage systems, as seen in Figure 7, which shows the discharge performance of several electrolyte formulations at 0 °C at a C/10 discharge rate from 4.8 to 2.0 V (cells were charged at room temperature prior to discharge).

Subsequently, LiBOB was incorporated into experimental electrolytes with the goal of enhancing the compatibility of the TPP-based formulations with high voltage systems. The combination of LiBOB and TPP into carbonate-based electrolytes and their optimization resulted in the identification of a JPL Generation #2 electrolyte that displays comparable reversible capacity and rate capability as the baseline electrolyte in an MPG-111-Li[LiNMC]O_2 (commercial Toda 9100 cathode) system. Preliminary assessments of the JPL Generation #2 electrolyte at high voltages indicate that there is no significant capacity or voltage benefit when the system is charged to 4.8 V versus to 4.6 V, as displayed in Figure 8. The cell with the baseline electrolyte delivered approximately 237 mAh when charged to 4.8 V and the cell with the JPL Generation #2 electrolyte delivered 231 mAh when charged to 4.6 V. A lower charge voltage may also provide better long-term cycling stability.

Future electrolyte development efforts will be focused on exploring the effects of higher concentrations of TPP and other flame-retardant additives, increasing the ionic conductivity of the electrolytes, gaining a fundamental understanding of the stabilizing effect of LiBOB at high voltages, and investigating other strategies to improve electrolyte compatibility in high voltage systems.

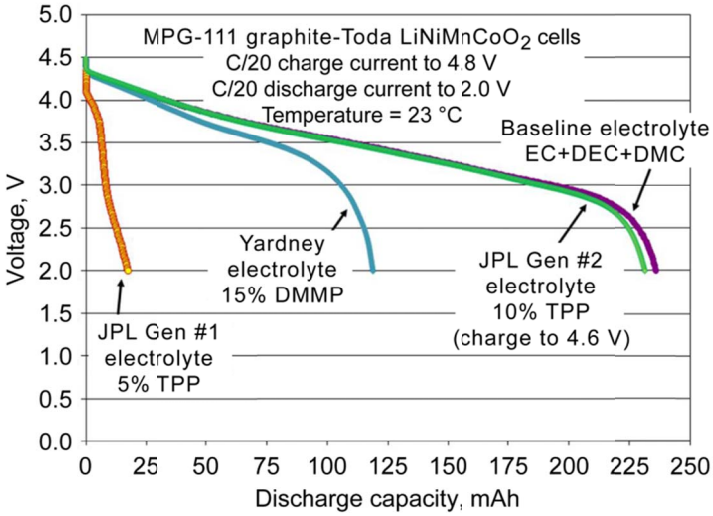

Figure 8.—Voltage versus capacity for different electrolyte formulations. Data was collected at NASA JPL.

2.3 Safety Devices

NASA's goals for inherent safety in the advanced HE and UHE cells dictate a need for cell-level technologies that are tolerant to electrical and thermal abuse such as over-temperature, overcharge, reversal, external short-circuit, and internal-shorts (meaning the cell designs pass internal short circuit tests) with no fire or thermal runaway. Under contract with NASA, Physical Sciences Incorporated (PSI) developed an approach to produce safer electrodes by utilizing a lithium cobalt phosphate ($LiCoPO_4$) coating on the cathode powders. This is discussed in more detail in References 2 and 10.

$LiCoPO_4$ coatings were applied to commercial Toda 9100 $Li[LiNMC]O_2$ cathode powders. Figure 9 shows the results of differential scanning calorimeter testing of the uncoated cathode powders and cathode powders that have been coated. The plots of coated materials are the results of the application of two different concentrations of the coating to the raw powders. As the figure shows, the coatings suppressed the exothermic peaks such that much less heat flow was generated as compared to the uncoated materials. The use of cathodes that have characteristically less heat flow could greatly reduce or eliminate the potential for thermal runaway associated with the cathode component in a full cell. Another key to the successful implementation of a safety component into a cell is measured by its ability to be effectively incorporated into the cell with minimal impact on the overall cell performance. Testing of uncoated and $LiCoPO_4$-coated commercial Toda 9100 $Li[LiNMC]O_2$ cathodes was performed in pouch cells of a nominal 1 Ah capacity containing a carbonaceous anode and the baseline electrolyte (defined in Section 2.1). First cycle formation is shown in Figure 10 for two cells with uncoated cathodes and two cells with coated cathodes. Cells were charged and discharged at C/20 between 4.6 and 2.8 V. The capacity delivered is quite similar for all the cells.

Preliminary test results indicate that the $LiCoPO_4$-coated cathodes may offer performance benefits during long term operation in cells. Figure 11 shows the cycling performance of a different set of pouch cells containing an uncoated and a $LiCoPO_4$-coated commercial Toda 9100 $Li[LiNMC]O_2$ cathode versus Li/Li+ while cycling at C/10 and room temperature. After formation, the coated cathode initially had lower specific capacity through about 20 cycles, however, it exhibited less fade and better cycling stability than the uncoated cathode.

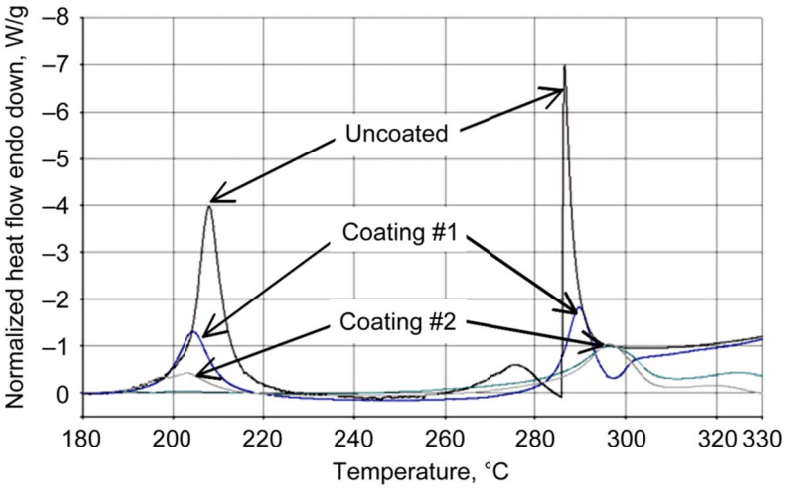

Figure 9.—DSC results showing heat flow versus temperature for uncoated and $LiCoPO_4$-coated $Li[LiNMC]O_2$ cathode materials. Data was collected at PSI.

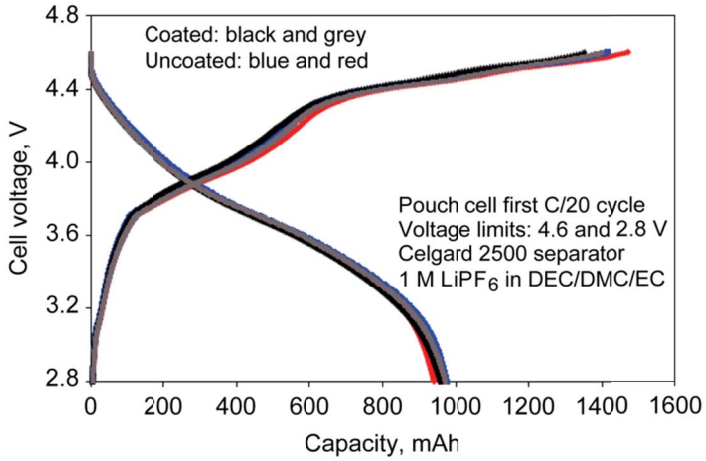

Figure 10.—Voltage versus capacity plots for the first formation cycle of pouch cells containing uncoated and $LiCoPO_4$-coated $Li[LiNMC]O_2$ cathode materials. Data was collected at PSI.

Although $LiCoPO_4$-coated cathodes have been evaluated in full pouch cells and tested for safety and long term electrical performance, the results were nonconclusive. The cells had low capacity and were constructed in a laboratory setting where reproducibility is challenging. In addition, a limited set of safety testing was performed to provide an early indication of the potential benefits of the coating, however, extensive testing that can provide conclusive evidence of the effectiveness of the coating in a full cell has not yet been carried out.

The extent to which these components may impact both safety and practical performance will continue to be evaluated in a full-cell configuration. Future efforts will focus on coating $Li[LiNMC]O_2$ powders with the PSI $LiCoPO_4$ coating, incorporating them into production full cells, and assessing the performance and safety of the cells in a more rigorous set of tests.

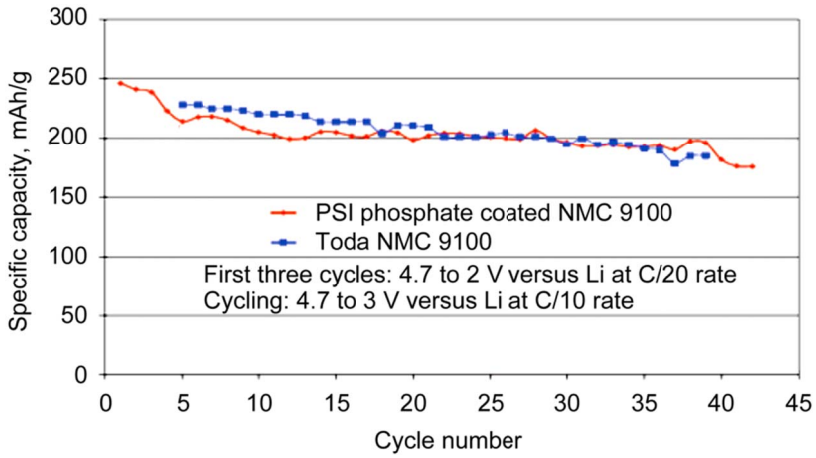

Figure 11.—Specific capacity while cycling at C/10 for pouch cells containing uncoated and $LiCoPO_4$-coated $Li[LiNMC]O_2$ cathode materials. Data was collected at Saft America.

3.0 Ultra High Energy Cell

3.1 Anodes

Advanced anodes are required for the success of the UHE cell. When coupled with a fully successful $Li[LiNMC]O_2$ cathode, approximately a three times increase in specific capacity is required over a SOA carbonaceous anode operating at like conditions. The goal for advanced anode materials is 1000 mAh/g at C/10 and 0 °C. Anode materials discussed in this paper were developed at Georgia Tech Research Corporation (GTRC) and Lockheed Martin Space Systems Company (LMSSC).

GTRC and LMSSC materials were independently assessed at NASA GRC using a standard set of test conditions in 2325-type coin cell half cells with a Li metal counter electrode, 1.0 M $LiPF_6$ in EC:DEC:DMC electrolyte in a 1:1:1 ratio by volume, and a 20 µm thick Tonen Setela separator. Formation procedures were recommended by the contractors who developed the materials. Since the anodes contain very different silicon:carbon (Si:C) ratios, binder types that range from elastomeric to rigid, and may include other conductive carbon additives, unique formation procedures for each material were developed through experimentation with the goals of formation of a good SEI layer, minimizing ICL, and maximizing capacity and cycling stability. Anode test procedures from GTRC and LMSSC are given in Table 4 and Table 5, respectively.

Key metrics that are fundamental to the overall operation of the anode have measured over the course of the past two years. The “best” values demonstrated for these parameters are compared to the goal values on the spider plot shown in Figure 12. Best values are defined as the highest value of the particular parameter achieved over the two year development period. Hence, values are not necessarily for the same material. Table 6 quantitatively lists the best and goal values and the materials from which the best values were measured. In addition, it lists the values of all the parameters for the most recent deliverables from each developer. Values reported are for the average of four cells. The parameters shown include reversible capacity, specific capacity, temperature performance, loading, rate capability, coulombic efficiency, and cycle life. The following paragraphs describe the data for these parameters in more detail.

TABLE 4.—GTRC ANODE TEST PROCEDURES[a]

Test stage	Test conditions
23 °C characterization	At 23 °C, charge at C/10 to 10 mV, hold voltage, and allow current to taper to C/50. Discharge at C/10 to 1.0 V. Perform for 10 cycles. Rest for 5 min after each charge and discharge.
0 °C characterization	All charges are performed at 23 °C. Charge at C/10 to 10 mV, hold voltage, and allow current to taper to C/50. Soak for 2 hr after all temperature changes. At 0 °C, discharge at C/10 to 1.0 V. Perform for 10 cycles.

[a]Deliverables 3 and 4

TABLE 5.—LMSSC ANODE TEST PROCEDURES[a]

Test stage	Test conditions
Formation	Perform at 23 °C. 1st cycle: Insert at C/20 to 25 mV, hold voltage and allow current to taper to C/50. De-insert to 0.9 V. 2nd cycle: Insert at C/8 to 150 mV, hold voltage and allow current to taper to C/50. De-insert to 0.9 V. Rest for 5 min after each complete insertion and de-insertion.
23 °C characterization	At 23 °C, charge at C/10 to 150 mV, hold voltage, and allow current to taper to C/50. Discharge at C/10 to 0.9 V. Perform for 10 cycles. Rest for 5 min after each charge and discharge.
0 °C characterization	All charges are performed at 23 °C. Charge at C/10 to 150 mV, hold voltage, and allow current to taper to C/50. Soak for 2 hr after all temperature changes. At 0 °C, discharge at C/10 to 0.9 V. Perform for 10 cycles.

[a]Deliverable 4

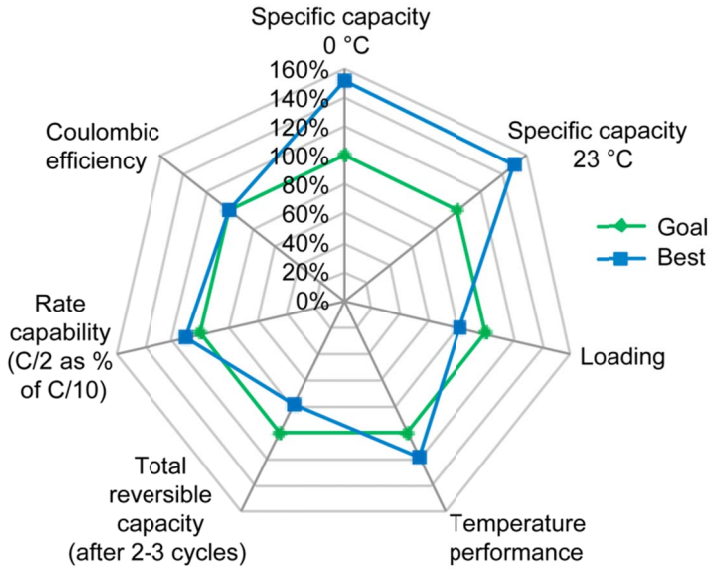

Figure 12.—Anode best values as compared to goal values.

TABLE 6.—SUMMARY OF ANODE BEST VALUES AND LATEST VALUES

Metric	Goal	Best values		Values for latest materials	
		Value	Material	GTRC 23 mo.	LMSSC 23 mo.
Total reversible capacity (after 2-3 cycles) (%)	89	70	GTRC 23 mo.	70	4
Specific capacity, RT, C/10 (mAh/g)	1110	1660	LMSSC 6 mo.	1598	1209
Specific capacity, 0 °C, C/10 (mAh/g)	1000	1528	GTRC 23 mo.	1528	1186
RT capacity retention at 0 °C (%)	90	107	GTRC 18 mo.	96	98
Loading (mAh/cm^2)	3.7	3.0	GTRC 11 mo.	0.9	2.7
Rate Capability at C/2 as compared to C/10 (%)	93	103	GTRC 18 mo.	94	81
Coulombic Efficiency (%)	99.5	98.8	GTRC 23 mo.	98.8	97.9
Projected Cycle Life (cycles to 80% of initial capacity)	250	~365 at C/2. 96% of initial capacity has been demonstrated through 130 cycles.	GTRC 23 mo.	~365 at C/2. 96% of initial capacity has been demonstrated through 130 cycles.	~23 at C/10

3.1.1 Reversible Capacity

Reversible capacity for anodes is measured after the second or third formation cycle (after the second cycle for the 23 mo. materials). The percentage of reversible capacity is equivalent to (100 percent minus the percentage of the cumulative ICL). The cumulative percent ICL is calculated by the formulas:

$$Cumulative\ ICL = \sum_{i=1}^{n} (charge_i - discharge_i)$$

$$Cumulative\ \%\ ICL = \frac{cumulative\ ICL}{discharge_n} \times 100$$

where n = number of cycles (n = 2 or 3), $charge_i$ = ith cycle insertion capacity, and $discharge_i$ = ith cycle deinsertion capacity.

The goal for cumulative reversible capacity of the anode is 89 percent, or inversely, the cumulative ICL should ideally be no greater than 11 percent. This value is based on the irreversible capacity of MPG-111 as measured by Saft America and independently confirmed by GRC. The results of NASA internal measurements show that the GTRC 23 mo. material exhibited a cumulative reversible capacity of 70 percent after the second formation cycle as compared to only 4 percent for the LMSSC 23 mo. material.

GTRC's initial average charge capacity (first formation cycle) was 2184 and 1739 mAh/g was delivered on discharge. On the second formation cycle 1827 mAh/g was inserted, and 1733 mAh/g was deinserted. As seen, the average percentage ICL on the second formation cycle improved to ~5 percent as compared to ~26 percent on the first cycle, resulting in a 30 percent cumulative percent ICL.

The LMSSC material attained a much higher specific insertion capacity on the first formation charge than the GTRC material, demonstrating an average of 3762 mAh/g. However, an average 35 percent ICL was measured for this cycle in which full insertion and de-insertion of Li was performed, almost 10 percent higher than the GTRC material. In subsequent cycles, LMSSC procedures called for voltage limits that allowed only partial insertion of Li. On the next cycle, an average of 1508 mAh/g was inserted, but only 1266 mAh/g was reversible, resulting in a 19 percent ICL on the second cycle and a cumulative ICL of 96 percent after the first two cycles.

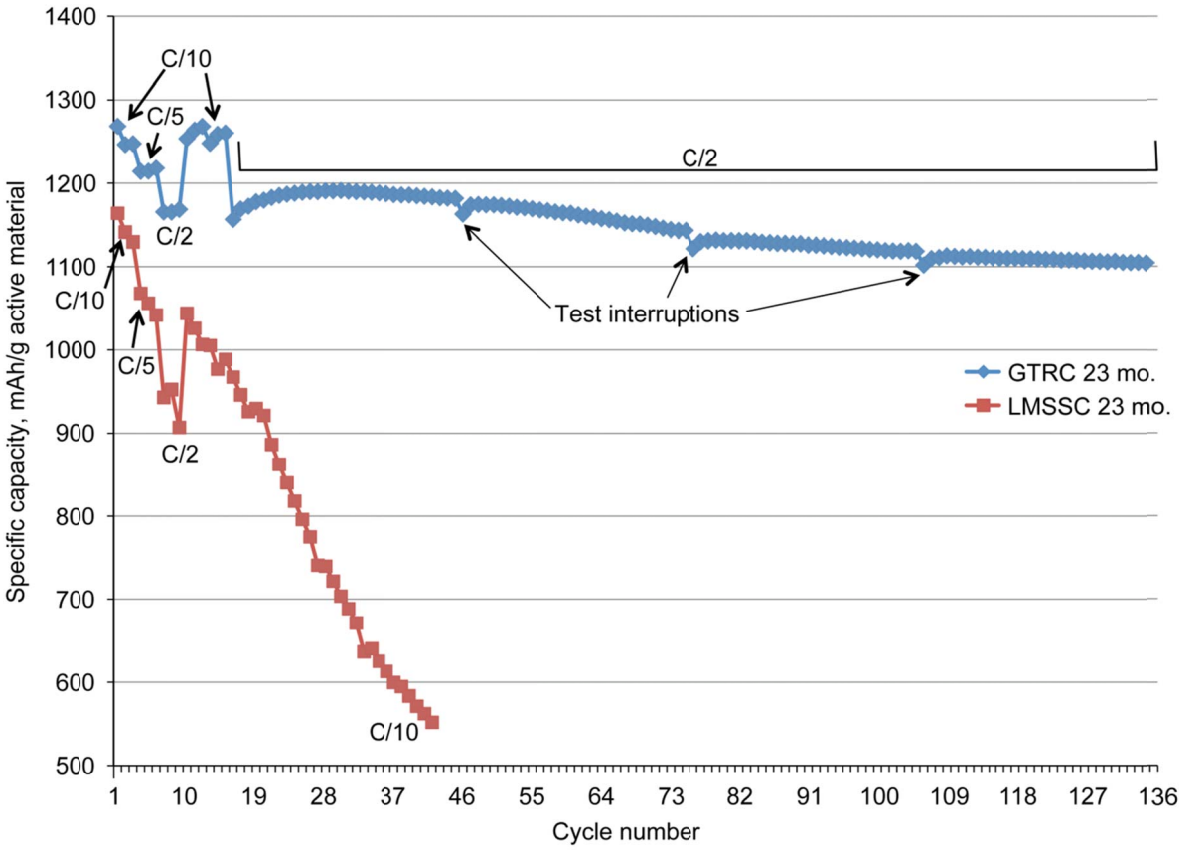

Figure 13.—Specific capacity versus cycle number for GTRC and LMSSC Si:C composite anodes. Data was collected at NASA GRC.

The extremely high irreversible capacity of the LMSSC anode beyond the first cycle is not a true capacity loss, but rather is induced by the cycling procedures adopted by LMSSC to avoid cycling outside of the amorphous range of Si (below 50 mV) and into the range in which Si is converted into its crystalline phase. LMSSC's internal studies showed that for their material composition, continuous cycling between the two phases (amorphous and crystalline) adversely impacted cycling stability and led to higher fade, as was initially reported by Obrovac and Krause (Ref. 11). However, cycling stability within the specified voltage limits as given in Table 5 is still poor on these materials, as seen in Figure 13. This cycling method precludes the materials' practical application in a lightweight cell, since the unusable capacity of the Si anode must still be carried and contributes to the mass of the cell. In addition, the cathode capacity must be matched to the initial Si capacity, which thereby increases the mass contribution of the cathode in the cell as well, even after the ICL of the cathode is accounted for.

3.1.2 Specific Capacity

Specific capacity at 23 and 0 °C are plotted as a percentage of the specific capacity goals at C/10 as measured between the voltage limits specified for each material (see Table 4 and Table 5) and at the respective temperature. Specific capacity at both 23 and 0 °C is reported for the first cycle following formation. For anodes, characterization at 0 °C is performed on a different set of cells than the 23 °C characterization is performed on to avoid any capacity fade introduced by prior cycling. Specific capacity at 0 °C is reported for discharge at 0 °C after a 23 °C charge.

LMSSC 6 mo. material demonstrated the best specific capacity of all of the developmental materials. Specific capacity measured at 23 °C and C/10 on this material is 1660 mAh/g, which far exceeded the goal value of 1110 mAh/g. However, the material had high ICL and poor rate capability. The GTRC

23 mo. material was a close second, achieving 1598 mAh/g. At 0 °C and C/10, 1528 mAh/g was obtained on the same material, which also far exceeded the 1000 mAh/g goal value. While this material exhibited excellent capacity retention at 0 °C, rate capability, and cycling stability, coulombic efficiency, ICL, and loading still need improvement. Project goals were established for 0 °C operation. Room temperature (RT) goals were calculated as the expected minimum specific capacity, based on the desire to retain at least 90 percent of RT capacity when operating at 0 °C.

3.1.3 Temperature Performance

Temperature performance is measured as the percentage of RT capacity retained at 0 °C. A goal of 90 percent was established for temperature performance based on what is reasonably practical given current SOA Li-ion cell performance. With the exception of the first set of deliverables from both contracts, all subsequent materials have demonstrated excellent temperature performance. The best values column in Table 6 indicates a value of 107 percent for the percentage of RT capacity retained at 0 °C since the capacity of the GTRC 23 mo. material tends to improve with cycling.

3.1.4 Loading

Loading is a measure of capacity per unit area. The target loading for the NASA anodes is ~3.7 mAh/cm^2. Currently the LMSSC and GTRC anodes have very low loading as compared to that found in practical cells that are designed to offer high capacity at moderate discharge rates. Low loading will necessitate larger electrode area to provide the equivalent capacity as electrodes with higher loading, which adversely impacts energy density. Specific energy will also suffer, as larger areas of current collector and possibly larger cell housings (i.e., inactive components) will be needed to accommodate impractically sized electrodes. Through our studies, trends showed that higher loaded anodes tended to have lower coulombic efficiency and cycle life. This is an area for further study and optimization.

3.1.5 Rate Capability

Rate capability testing is performed at C/5 and C/2 and compared to specific capacity achieved at C/10. A target of 93 percent of the C/10 performance was established for C/2 performance. The Si:C-based anodes have demonstrated excellent rate capability. The rate capability for recent deliverables has consistently measured between 94 and >100 percent (the specific capacity of the GTRC 23 mo. material improved with cycling).

3.1.6 Cycle Life

Cycle life assessments are performed at 23 °C in half-cells vs. Li/Li+. The goal for the UHE cell is 200 cycles at 100 percent DoD to 80 percent of initial capacity when cycled at C/2. To attain 200 cycles on the cell level, 250 cycles is desired from the components. Cycle life of the LMSSC material is assessed at C/10 due to the high fade observed in early cycling. Figure 13 shows results of cycle life testing for GTRC and LMSSC 23 mo. materials. Here, initial capacity is defined as the capacity delivered on the first discharge of continuous cycling (cycle 10 for the LMSSC material and cycle 16 for the GTRC material). The LMSSC material displays poor cycling stability, achieving only 23 cycles to our defined point of failure. Further, it only achieves 37 cycles prior to its specific capacity falling below the anode threshold value of 600 mAh/g, the minimum success criteria. The GTRC material demonstrated >45 cycles with virtually no fade, and as previously discussed, the specific capacity tended to improve with cycling. Ninety-six percent of the initial capacity is measured after 130 cycles. Cycling on this material is still in progress. Using a linear extrapolation based on the rate of fade, approximately 365 cycles are projected to 80 percent of the initial capacity.

In order to improve cycling stability of the Si-based anodes, <10 percent by weight of VC was added to the baseline electrolyte in both GTRC and LMSSC cells. While a beneficial effect on cycling stability was seen in the GTRC material, the performance of the LMSSC material did not improve with the addition of VC.

3.1.7 Discussion

Figure 14 and Figure 15 contain spider plots that show the progression of the parameters discussed above for 6, 11, 18, and 23 mo. materials from GTRC and LMSSC. Values plotted in each graph pertain to a single material. NASA has demonstrated excellent performance with these NRA-developed Si-based anode materials when performance is measured based on specific capacity at 23 and 0 °C, temperature performance, rate capability and cycling stability metrics. For the GTRC materials, improvements to IC, coulombic efficiency, and loading remain as challenges to be addressed further.

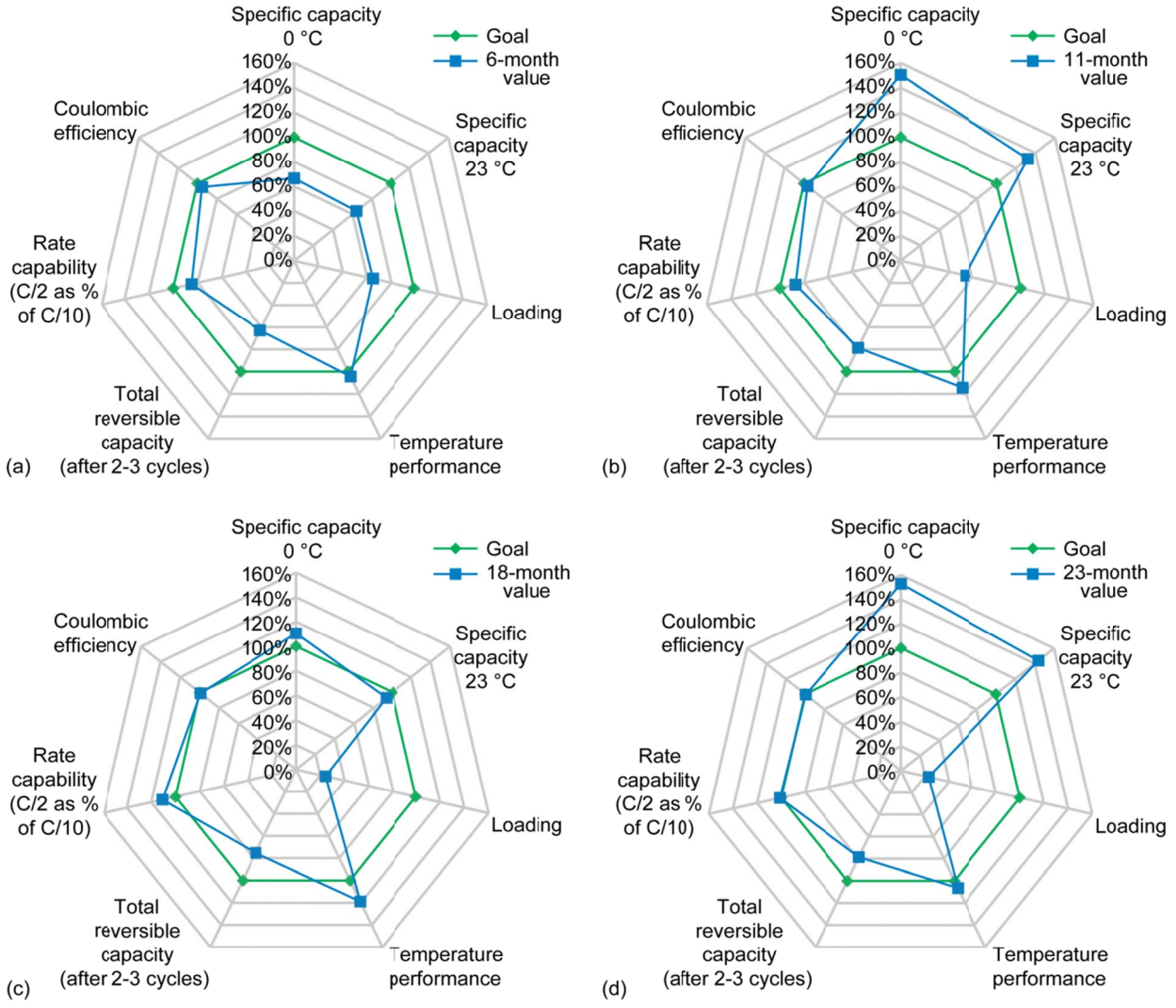

Figure 14.—Values of GTRC key anode parameters as a function of elapsed time into development. (a) Results after 6 months of development. (b) Results after 11 months of development. (c) Results after 18 months of development. (d) Results after 23 months of development.

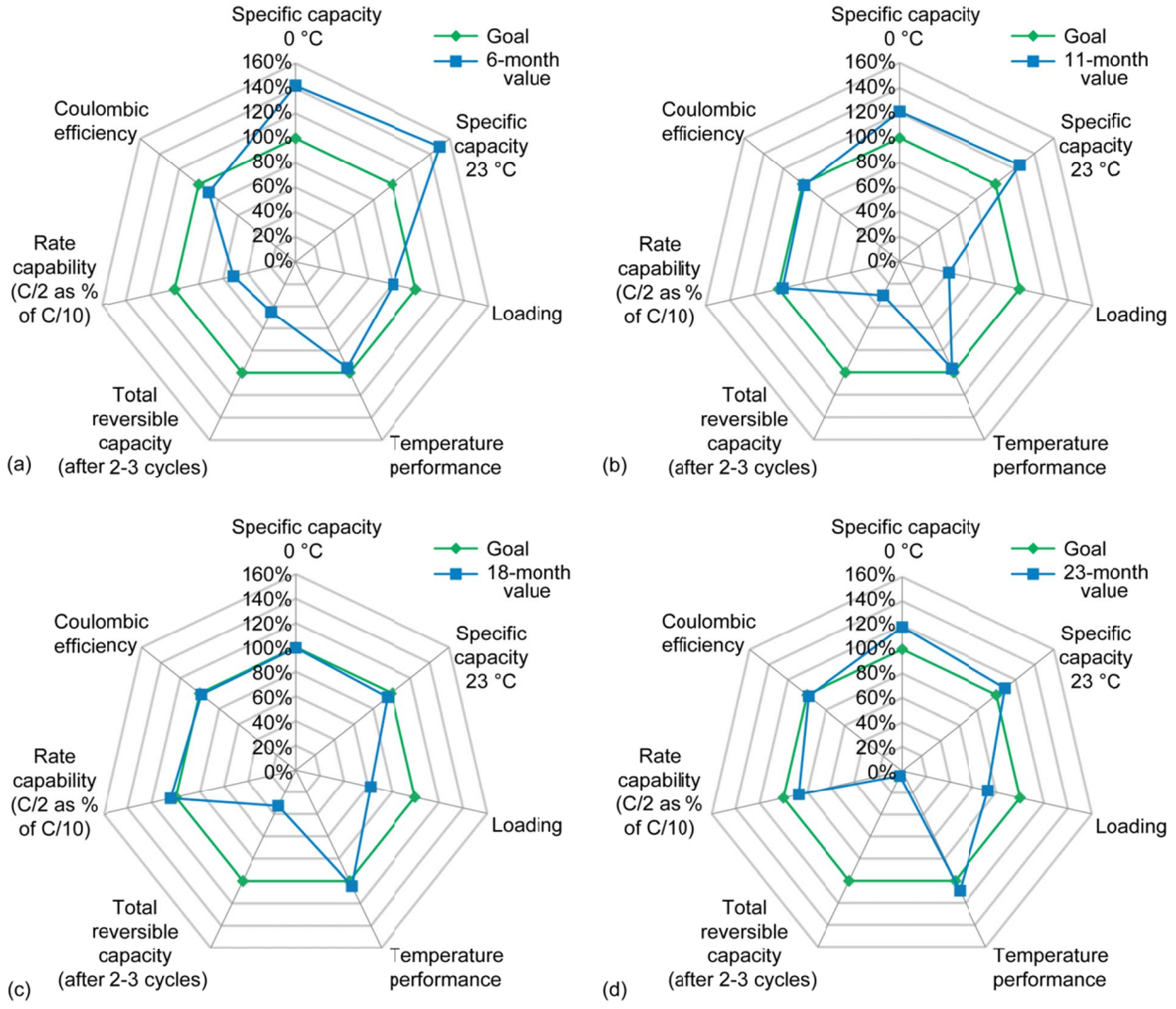

Figure 15.—Values of LMSSC key anode parameters as a function of elapsed time into development. (a) Results after 6 months of development. (b) Results after 11 months of development. (c) Results after 18 months of development. (d) Results after 23 months of development.

As discussed in the section on reversible capacity, the incorporation of the LMSSC anode in a cell would require the use of cycling regimes that limit the useable capacity in the cell, thereby resulting in large mass penalties. Upon modeling its practical application in an integrated cell design, the LMSSC anode was eliminated from further consideration in the UHE cell.

4.0 Cell Projections

Cell-level specific energy and energy density values are predicted using the cathode and anode materials that provide the best combination of high specific capacity and high capacity retention to date. Projected values for cell level specific energy and energy density are based on projections using data for the most promising materials' performance at C/10 to 3.0 V and 0 °C (Ref. 12). The goal values versus the projected values are shown in Figure 16. Performance of Li-ion cells from the 2003 Mars Exploration Rover batteries is also included for comparison. These cells contain the chemistry that this development project uses as a baseline to measure progress.

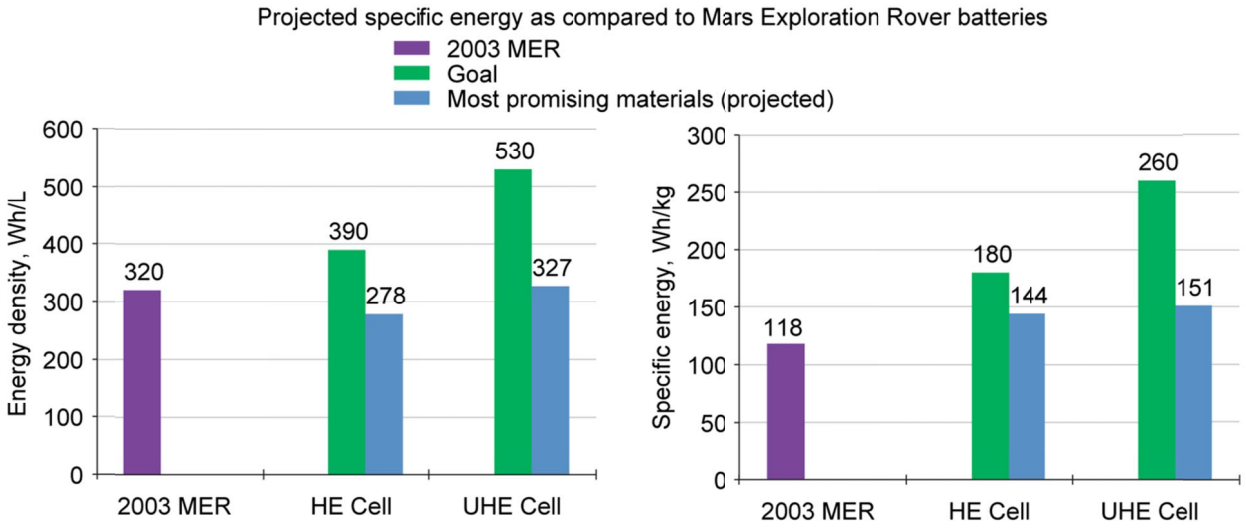

Figure 16.—HE and UHE cell projected specific energy and energy density as compared to goal values at C/10 and 0 °C to 3.0 V.

When projecting performance on a cell level, integration issues between the anode and cathode were considered. Poor performance of the NMC cathodes at 0 °C also translates into significant cell-level performance penalties at 0 °C. Additionally, as discussed in Reference 12, Si-based anodes produce a lower and more sloping discharge profile in a cell than graphite anodes, resulting in significant capacity below 3.0 V. Ultimately, the developmental anode or cathode must also be loaded such that it can match the capacity of the electrode it is being paired with. Attaining higher loadings has been challenging with some of the developmental materials, and may be detrimental to other aspects of the materials' performance. These and other integration issues are among challenges to be addressed as the project moves toward building cells. They are currently being addressed through cell design modeling, performance modeling, electrolyte optimization, component compatibility trials, and additional fundamental research efforts that target specific characteristics of material improvement and optimization.

5.0 Summary

Steady progress in the development of advanced components for safe, lightweight, and compact HE and UHE Li-ion cells for NASA's Exploration applications has been achieved over the past 2 years. As discussed in this paper, in each of the component areas, additional development work is still required to achieve full success with the materials and bring them to maturity for use in production cells. Additionally, the combination of the parameters described above that meets or exceeds our goals in a singular cathode and a singular anode system is necessary for full success of the electrode materials and their suitability for incorporation into practical cells.

Electrolytes that are compatible with the components are also required. For HE cells, electrolytes containing a combination of LiBOB and TPP have demonstrated an ideal combination of flame-retardant properties, high voltage stability, and reversible capacity. For UHE cells, electrolytes that are compatible with Si-based electrodes and that facilitate stable SEI layer formation on these novel materials are under investigation.

$LiCoPO_4$ coatings have been shown to improve the thermal properties of $Li[LiNMC]O_2$ cathode powders on the component level. Safety testing of higher capacity, representative cells containing these materials is required in order to assess their safety benefits in an integrated Li-ion system.

Appendix—Nomenclature

°C	degrees Celsius
C	carbon
DEC	diethyl carbonate
DMC	dimethyl carbonate
DMMP	dimethyl methyl phosphonate
DoD	depth-of-discharge
EC	ethylene carbonate
EMC	ethyl methyl carbonate
g/cc	grams per cubic centimeter
GRC	Glenn Research Center
GTRC	Georgia Tech Research Corporation
HE	High Energy
ICL	irreversible capacity loss
JPL	Jet Propulsion Laboratory
JSC	Johnson Space Center
KPP	key performance parameters
LiBOB	lithium bis(oxalato) borate
$LiCoPO_4$	lithium cobalt phosphate
Li-ion	lithium-ion
$LiPF_6$	lithium hexafluorophosphate
LMSSC	Lockheed Martin Space Systems Company
$Li[LiNMC]O_2$	lithium nickel manganese cobalt oxide
M	molar
mAh/g	milliampere-hours per gram
MCMB	mesocarbon microbeads
MER	Mars Exploration Rovers
mo.	month(s)
mV	millivolts
NASA	National Aeronautics and Space Administration
NEI	NEI Corporation
PSI	Physical Sciences, Incorporated
RT	room temperature
SEI	solid electrolyte interface
SET	self-extinguishing time
Si	silicon
Si:C	silicon:carbon
SOA	state-of-the-art
TD	tap density

TPP	triphenyl phosphate
UHE	Ultra High Energy
μm	micrometer
UTA	University of Texas at Austin
V	volts
VC	vinylene carbonate
Wh/kg	watt-hours per kilogram
Wh/L	watt-hours per liter
YTP/URI	Yardney Technical Products/University of Rhode Island

References

1. C.M. Reid and W.R. Bennett, "A Study on Advanced Lithium-Based Battery Cell Chemistries to Enhance Lunar Exploration Missions," National Aeronautics and Space Administration Glenn Research Center, Cleveland, OH, NASA/TM—2010-216791, September 2010.
2. C.M. Reid, "Progress in Materials and Component Development for Advanced Lithium-ion Cells for NASA's Exploration Missions," National Aeronautics and Space Administration Glenn Research Center, Cleveland, OH, NASA/TM—2011-217209, September 2011.
3. A. Manthiram, High-energy density cathodes for next generation lithium-ion batteries, Final Report to NASA Glenn Research Center from The University of Texas at Austin for contract NNC09CA08C, March 2011.
4. N.M. Hagh, F. Badway, M. Moorthi, G. Skandan, W. West, R. Bugga, C. Reid, Improvements in Energy Density and Stability of Advanced Cathode Materials for NASA's Applications, *NASA Aerospace Battery Workshop*, November 16-18, 2010.
5. J. Li, R. Klopsch, M.C. Stan, S. Nowak, M. Kunze, M. Winter, and S. Passerini, Synthesis and electrochemical performance of the high voltage cathode material $Li[Li_{0.2}Mn_{0.56}Ni_{0.16}Co_{0.08}]O_2$ with improved rate capability, J. Power Sources, 196 (2011) 4821-4825.
6. N.M. Hagh, F. Badway, K. Martin, M. Moorthi, and G. Skandan, High Energy Density Cathode Materials for Li-Ion Battery Applications, *44th Power Sources Conference*, Las Vegas, NV, June 14-17, 2010.
7. N.M. Hagh, G.G. Amatucci, A new solid-state process for synthesis of $LiMn_{1.5}Ni_{0.5}O_{4-\delta}$ spinel, J. Power Sources, 195 (2010) 5005-5012.
8. J.M. Zheng, X.B. Wu, and Y. Yang, A comparison of preparation method on the electrochemical performance of cathode material $Li[Li_{0.2}Mn_{0.54}Ni_{0.13}Co_{0.13}]O_2$ for lithium ion battery, Electrochimica Acta 56 (2011) 3071-3078.
9. M.C. Smart, F.C. Krause, W.C. West, J. Soler, L. Whitcanack, and R.V. Bugga, "Development of Electrolytes With Improved Safety Characteristics," *Final FY10 Report for the NASA Exploration Technology Development Program Energy Storage Project,* September, 2010.
10. C.M. Lang, A. Newman, K. Constantine, and J. Ma, Improved Cathode Material Safety via a Metal Phosphate Coating, *NASA Aerospace Battery Workshop,* Huntsville, AL, November, 2009.
11. M.N. Obrovac and L.J. Krause, Reversible Cycling of Crystalline Silicon Powder, J. Electrochem. Soc. 154 (2007) A103-A108.
12. W.R. Bennett, "Forecasts for Hypothetical Li-Ion Cells Using FY2010 Data for ETDP Electrodes," National Aeronautics and Space Administration Glenn Research Center, Cleveland, OH, NASA/TM—2011-TBD, 2011 (to be published).
13. R. Staniewicz, personal communication, September 2011.
14. J. Liu, Q. Wang, B. Reeja-Jayan, and A. Manthiram, Carbon-coated high capacity layered $Li[Li_{0.2}Mn_{0.54}Ni_{0.13}Co_{0.13}]O_2$ cathodes, Electrochemistry Communications, 12 (2010) 750-753.

REPORT DOCUMENTATION PAGE		Form Approved OMB No. 0704-0188

1. REPORT DATE *(DD-MM-YYYY)*	2. REPORT TYPE	3. DATES COVERED *(From - To)*
01-09-2012	Technical Memorandum	

4. TITLE AND SUBTITLE
Advanced Materials and Component Development for Lithium-Ion Cells for NASA Missions

5a. CONTRACT NUMBER

5b. GRANT NUMBER

5c. PROGRAM ELEMENT NUMBER

6. AUTHOR(S)
Reid, Concha, M.

5d. PROJECT NUMBER

5e. TASK NUMBER

5f. WORK UNIT NUMBER
WBS 152964.04.01.01.01.03

7. PERFORMING ORGANIZATION NAME(S) AND ADDRESS(ES)
National Aeronautics and Space Administration
John H. Glenn Research Center at Lewis Field
Cleveland, Ohio 44135-3191

8. PERFORMING ORGANIZATION REPORT NUMBER
E-18372

9. SPONSORING/MONITORING AGENCY NAME(S) AND ADDRESS(ES)
National Aeronautics and Space Administration
Washington, DC 20546-0001

10. SPONSORING/MONITOR'S ACRONYM(S)
NASA

11. SPONSORING/MONITORING REPORT NUMBER
NASA/TM-2012-217689

12. DISTRIBUTION/AVAILABILITY STATEMENT
Unclassified-Unlimited
Subject Categories: 15, 20, and 44
Available electronically at http://www.sti.nasa.gov
This publication is available from the NASA Center for AeroSpace Information, 443-757-5802

13. SUPPLEMENTARY NOTES

14. ABSTRACT
Human missions to Near Earth Objects, such as asteroids, planets, moons, liberation points, and orbiting structures, will require safe, high specific energy, high energy density batteries to provide new or extended capabilities than are possible with today's state-of-the-art aerospace batteries. The Enabling Technology Development and Demonstration Program, High Efficiency Space Power Systems Project battery development effort at the National Aeronautics and Space Administration (NASA) is continuing advanced lithium-ion cell development efforts begun under the Exploration Technology Development Program Energy Storage Project. Advanced, high-performing materials are required to provide improved performance at the component-level that contributes to performance at the integrated cell level in order to meet the performance goals for NASA's High Energy and Ultra High Energy cells. NASA's overall approach to advanced cell development and interim progress on materials performance for the High Energy and Ultra High Energy cells after approximately 1 year of development has been summarized in a previous paper. This paper will provide an update on these materials through the completion of 2 years of development. The progress of materials development, remaining challenges, and an outlook for the future of these materials in near term cell products will be discussed.

15. SUBJECT TERMS
Lithium batteries; Storage batteries; Electric batteries; Electrochemical cells; Energy storage; Space missions; Spacecraft power supplies; Electric power supplies

16. SECURITY CLASSIFICATION OF:			17. LIMITATION OF ABSTRACT	18. NUMBER OF PAGES	19a. NAME OF RESPONSIBLE PERSON
a. REPORT	b. ABSTRACT	c. THIS PAGE			STI Help Desk (email:help@sti.nasa.gov)
U	U	U	UU	32	19b. TELEPHONE NUMBER *(include area code)* 443-757-5802